

# Fabrication and properties of alginate/calcium phosphate hybrid beads: A comparative study

著者	Tripathi Garima, Miyazaki Toshiki
journal or publication title	Bio-Medical Materials and Engineering
volume	32
number	1
page range	15-27
year	2021-01-21
URL	<a href="http://hdl.handle.net/10228/00008014">http://hdl.handle.net/10228/00008014</a>

doi: <https://doi.org/10.3233/BME-206012>

**Fabrication and properties of alginate / calcium phosphate hybrid beads: A comparative study**

Garima Tripathi\* and Toshiki Miyazaki\*

Graduate School of Life Science and Systems Engineering, Kyushu Institute of Technology,  
2-4, Hibikino, Wakamatsu-ku, Kitakyushu 808-0196, Japan

Corresponding author:

\*Garima Tripathi and Toshiki Miyazaki

Graduate School of Life Science and Systems Engineering, Kyushu Institute of Technology,  
2-4, Hibikino, Wakamatsu-ku, Kitakyushu 808-0196, Japan

Tel/Fax: +81-93-695-6025

E-mail: tgarima910@gmail.com (G.T.) / tmiya@life.kyutech.ac.jp (T.M.)

## **Abstract**

Microbeads for bone repair have been widely studied because they can be conveniently used in clinical applications. This study concerns the preparation, physical properties and *in vitro* characterisation of different types of alginate / calcium phosphate (CaP) ceramic microbeads, which were designed for use as drug delivery systems and bone-regeneration matrices. Hybrid microbeads were successfully prepared from sodium alginate and various CaP, namely  $\alpha$ -tricalcium phosphate,  $\beta$ -tricalcium phosphate and hydroxyapatite using the liquid droplet method. Porosity, swelling properties and *in vitro* degradation of the microbeads in aqueous environment were significantly changed by the added CaP. The compressive strength of the blocks fabricated from the beads was around 120 MPa irrespective of the type of CaP. The initial release rate of the model drug methylene blue was suppressed by the addition of CaP. The alginate-CaP composite beads hold promising potential as an encapsulation carrier of drugs and component of bone substitutes.

**Keywords:** Alginate, Calcium phosphate, Microbeads, *in vitro* drug release, *in vitro* degradation

## 1. Introduction

Calcium phosphates (CaP) are recognized as a useful biomaterial in hard tissue regeneration [1] because of their osteoconductivity and efficacy in most clinical applications in orthopaedics and dentistry[2] . Hydroxyapatite (HAp;  $\text{Ca}_{10}(\text{PO}_4)_6(\text{OH})_2$ ) exhibits excellent biocompatibility because of its similarity in composition to natural bone [3]. Apart from HAp,  $\alpha$ -tricalcium phosphate ( $\alpha$ -TCP;  $\alpha\text{-Ca}_3(\text{PO}_4)_2$ ) and  $\beta$ -tricalcium phosphate ( $\beta$ -TCP;  $\beta\text{-Ca}_3(\text{PO}_4)_2$ ) have been widely studied as materials for bone repair owing to their outstanding biocompatibility, bioactivity and high osteoconductivity. For all forms of bone graft, a spherical shape of the material could be useful for uniform packing in sporadically shaped defects [4] .

Researchers have recently focused heavily on the binding of ceramic bone grafts with bioactive molecules for osteoinductivity and osteogenesis [5], and on refining osteogenic properties of bone grafts used for bony defects. The binding of biomolecules to ceramics that allows a controlled release of the laden biomolecules via the binding mode has proved difficult. Numerous biomaterials and their derivatives such as alginate [6-7], chitosan [8-9], agarose [10-11], gelatin [12-13], collagen[14-15] and fibroin[16] have been studied for regeneration of osteochondral interfaces or articular cartilage tissues because of their inherent biocompatibility, non-toxicity and biodegradability.

Although natural materials allow favourable biological interactions with host tissues, the low mechanical strength and instability of the materials compared with the native cartilage sometimes complicate their clinical applications [17]. Alginate is considered to be biocompatible, non-toxic; non-immunogenic and biodegradable. Given its natural abundance and low cost, it has been widely used as thickener and emulsifying agent in the food industry and as tissue engineering material. The choice of alginate as a polymeric vehicle can be attributed to its favourable properties and versatility. Sodium alginate and most other alginates from monovalent metals are soluble in water, forming solutions of considerable

viscosity. Alginate can be easily modified in any form such as hydrogels, microbeads, microcapsules, sponges, foams and fibres, allowing increased applications in various fields such as tissue engineering and drug delivery. Alginate can be chemically or physically modified for tuning of its biodegradability, mechanical strength, gelation property and cell affinity towards respective applications [18].

Various alginate-CaP hybrids have been developed as synergetic systems for bone regeneration in the form of microspheres [4], cement [19,20], bulk porous scaffold [21-23]. In the case of microsphere preparation, HAp and calcium titanium phosphate were selected as an inorganic phase and enzyme release was evaluated [4]. However, no comparative studies of alginate-based hybrid beads with various CaP such as HAp,  $\alpha$ -TCP and  $\beta$ -TCP prepared by the same experimental conditions have been reported on applications in interfacial osteochondral defects or drug delivery vehicles for hard tissue regeneration. In addition, although several hybrid microspheres have been developed from CaP and polylactide, a representative synthetic biodegradable polymer [24,25], effects of CaP have not been sufficiently revealed. If such points are clarified, it is expected that fundamental design for the hybrids with varied biological properties and drug delivery ability can be established.

In our pursuit, we performed a comparative study by combining  $\alpha$ -TCP,  $\beta$ -TCP or HAp with sodium alginate, a natural polysaccharide that has been shown to be biocompatible. This work describes the preparation and initial characterisation of the alginate microbeads with and without CaP, designed as injectable drug delivery matrices and bone filling materials.

## **2. Materials and methods**

### *2.1. Materials*

Sodium alginate, calcium chloride ( $\text{CaCl}_2$ ), methylene blue were purchased from Wako Pure Chemical Industries, Ltd., Osaka, Japan.  $\alpha$ -Tricalcium phosphate ( $\alpha$ -TCP-B) and  $\beta$ -tricalcium phosphate ( $\beta$ -TCP-100) were purchased from Taihei Chemical Industrial Co., Osaka, Japan and HAp was purchased from Central Glass Co., Ltd., Tokyo Japan. Ultrapure water (prepared using Direct-Q, Nihon Millipore K.K., Tokyo, Japan) was employed for experimental purposes.

### *2.2. Preparation of alginate and alginate hybrid beads*

Sodium alginate was dissolved in deionized water to a final concentration of 4% (w/v) with and without equal weight ratio of  $\alpha$ -TCP,  $\beta$ -TCP or HAp. Pure and hybrid alginate beads were prepared by dripping the 4 mass% sodium alginate solution into  $\text{CaCl}_2$  under constant stirring at room temperature. The droplets were left for 1 hour in the gelling bath before being removed and rinsed with distilled water.

### *2.3. Material characterisation*

The surface structural changes of the samples were characterised using a scanning electron microscope (SEM; Model S-3500N; Hitachi Co., Tokyo, Japan), an energy dispersive X-ray analyser (EDX; Model EX-400; Horiba Co., Kyoto, Japan), X-ray diffractometer (XRD; MXP3V; Mac Science Ltd., Yokohama, Japan) and Fourier-transform infrared spectrometer (FT-IR, FT/IR-6100, JASCO Co., Tokyo, Japan). For FT-IR, the gels were first pulverised and mixed with KBr powder at a mass ratio of 1:100. A thin film was prepared by uniaxially pressing the mixed powder to measurement.

### *2.4. Porosity and density measurements*

The density and porosity of the prepared samples were measured by water displacement. A sample with a known weight  $w_1$  was immersed in a beaker holding a known volume  $v_1$  of water. A series of brief evacuation-repressurisation cycle were performed to force the water into the samples. Then the total volume of the water plus the water-impregnated samples ( $v_2$ ) and the volume of the residual water after the water-impregnated samples were removed ( $v_3$ ) were recorded. The density of the sample ( $d$ ) and the porosity of the sample ( $\epsilon$ ) are expressed as follows:

$$d = w_1 / (v_2 - v_3) \text{-----(1)}$$

$$\epsilon = (v_1 - v_3) / (v_2 - v_3) \times 100 \text{-----(2)}$$

### 2.5. Swelling ratios of beads

The weights of the dried beads and beads immersed in deionized water for 48 h at room temperature were determined. In brief, the pre-weighed, dried hybrid beads were immersed in 50 ml of ultrapure water at 25 °C for 24 h. At a regular time interval (1 h), the hybrid beads were taken out from ultrapure water, the surface water was blotted off with tissue paper and then reweighed. The experiment was carried out until the equilibrium weights of the films were reached. The swelling ratio was evaluated using:

$$\text{Swelling ratio (\%)} = (W_s - W_d) / W_d \times 100 \text{-----(3)}$$

where  $W_s$  is the weight of the water-swollen beads and  $W_d$  is the weight of the dried beads.

### 2.6. In vitro degradation

The alginate/alginate hybrid hydrogels were incubated in 20.0 ml of saline solution at 37 °C. Gel degradation behaviour was monitored by measuring the dry weight loss over time. At least four samples at each time point were used to obtain the weight loss curve. Experiments were done under sterile conditions to prevent bacterial and fungal contamination.

### *2.7. Mechanical properties*

The mechanical strength of the samples was evaluated in terms of compressive strength. For the purpose, we used moulds made with cylindrical cavities in silicon rubber sheets of the preferred thickness. Afterwards we coated the outer layer with 50 mass% polyacrylic acid solution and immediately filled the cavity with the granules, and left it to dry completely for 2 days. The completely dried samples were pulled out from the silicon sheet. The diameter and height of each sample were first measured with a digital micrometre (IP65, Mitutoyo Co., Ltd., Kanagawa, Japan). Each sample was crashed at a crosshead speed of 1 mm/min using a universal testing machine (Autograph AGS-J, Shimadzu, Kyoto, Japan). The average of eight samples was taken as the value of compressive strength.

### *2.8. In vitro release of model drug*

Methylene blue was used as a model drug to evaluate the performance of the calcium alginate beads in controlled drug delivery. Thirty samples of calcium alginate beads were equilibrated in a 30-ml methylene blue solution (500 mg/ml) for 24 hours. The beads were rinsed thrice before the drug release studies. The release profile of methylene blue was studied using a UV-Vis spectrophotometer. The concentration of methylene blue was determined spectrophotometrically at 664.5 nm.

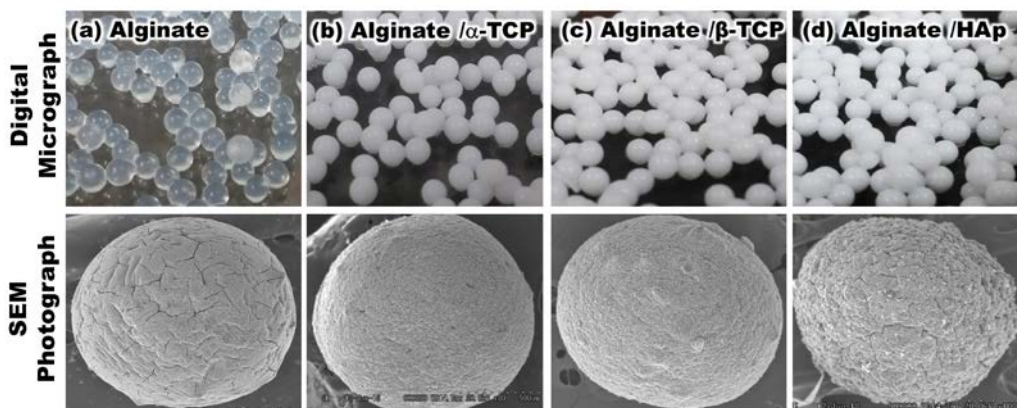
### *2.9. Statistical analysis*



All values were analysed by one-way analysis of variance followed by Turkey's multiple comparison tests. Significant differences were assumed at  $p < 0.05$ .

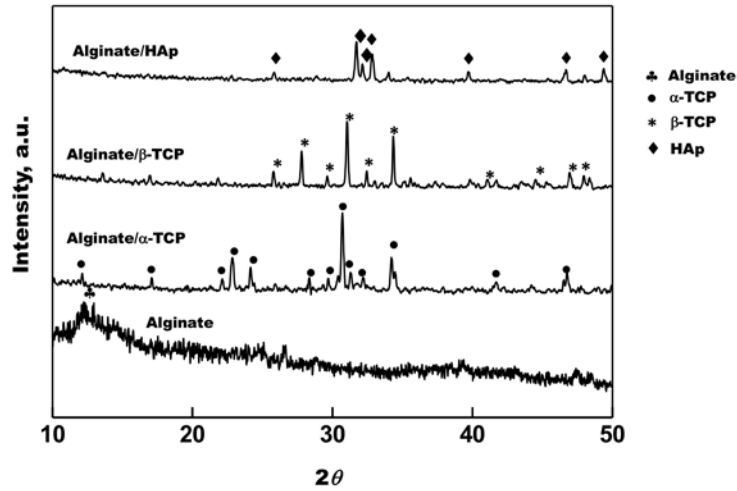
### 3. Results

Figure 1 illustrates the typical optical and SEM photographs of the prepared beads. There were no significant differences in the shape and size of the granules at macroscopic level. However, at higher magnification differences could be clearly observed in terms of roughness and shape. Alginate and Alginate/HAp showed numerous cracks.



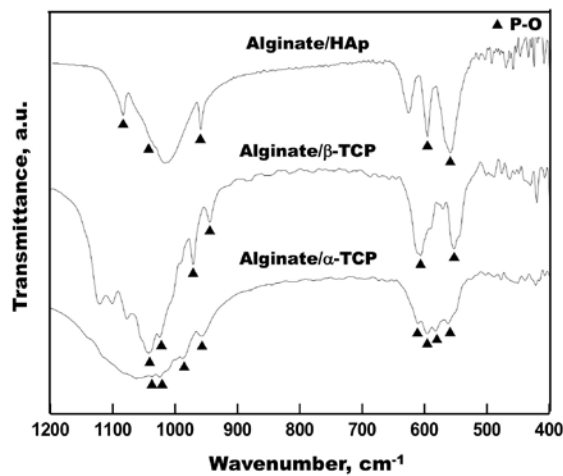
**Figure 1** Digital photographs and SEM images of the prepared beads after drying.

Figure 2 shows the XRD patterns of the prepared beads. Alginate showed a broad peak at  $2\theta=13.7^\circ$ , consistent with its amorphous nature [26,27]. The other samples demonstrated peaks corresponding to each CaP ( $\alpha$ -TCP: JCPDS card 9-348,  $\beta$ -TCP: JCPDS card 9-169 and HAp: JCPDS card 9-432). There were no other foreign peaks in any of the samples.



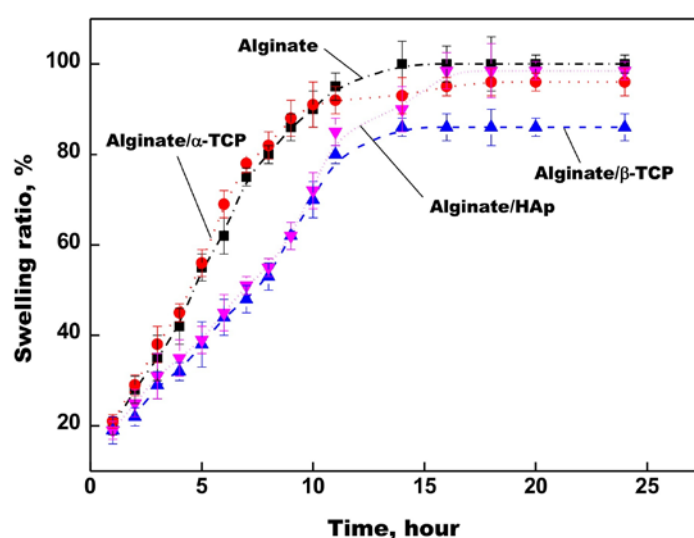
**Figure 2** XRD patterns of the prepared beads after drying.

Figure 3 presents the FT-IR spectra of Alginates/ $\alpha$ -TCP, Alginates/ $\beta$ -TCP and Alginates/HAp hybrid beads. Peaks of P-O characteristic of CaP were observed for all the samples around 550–500 and 950–1050  $\text{cm}^{-1}$  [28,29]. According to Ma *et al.*, HAp should have a strong absorption band around 1035  $\text{cm}^{-1}$  due to the stretching of  $\text{PO}_4^{3-}$  [28]. However, it is well known that sodium alginate also has a strong absorption band of C–O–C at this wavenumber [30]. Thus, the observed P-O band of Alginates/HAp around 1035  $\text{cm}^{-1}$  would be very weak.



**Figure 3** FT-IR spectra of Alginates/ $\alpha$ -TCP, Alginates/ $\beta$ -TCP and Alginates/HAp beads after drying.

Swelling behaviour is a very important property of a drug delivery vehicle, because it has a great influence on the control of drug release. Figure 4 describes the swelling ratio of the samples in ultrapure water at 37 °C. The hybrid beads reached their equilibrium swelling state at around 15 hours. In the first 12 hours, the swelling ratio decreased in the order: Alginate~Alginate/ $\alpha$ -TCP>Alginate/HAp~Alginate/ $\beta$ -TCP. After 24 hours, it decreased in the order: Alginate>Alginate/HAp>Alginate/ $\alpha$ -TCP>Alginate/ $\beta$ -TCP.



**Figure 4** Swelling ratio of the prepared beads after immersion in ultrapure water for various periods (n=3).

Figure 5 describes the density and porosity of the prepared samples. The density decreased in the order: Alginate/HAp>Alginate/ $\beta$ -TCP>Alginate/ $\alpha$ -TCP>Alginate. The porosity of Alginate was around 65%, while those of the other samples were around 30% irrespective of the kind of CaP. There were distinct differences in the density and porosity among the samples. The added CaP was assumed to fill the pores in the alginate matrix, thereby reducing the porosity.

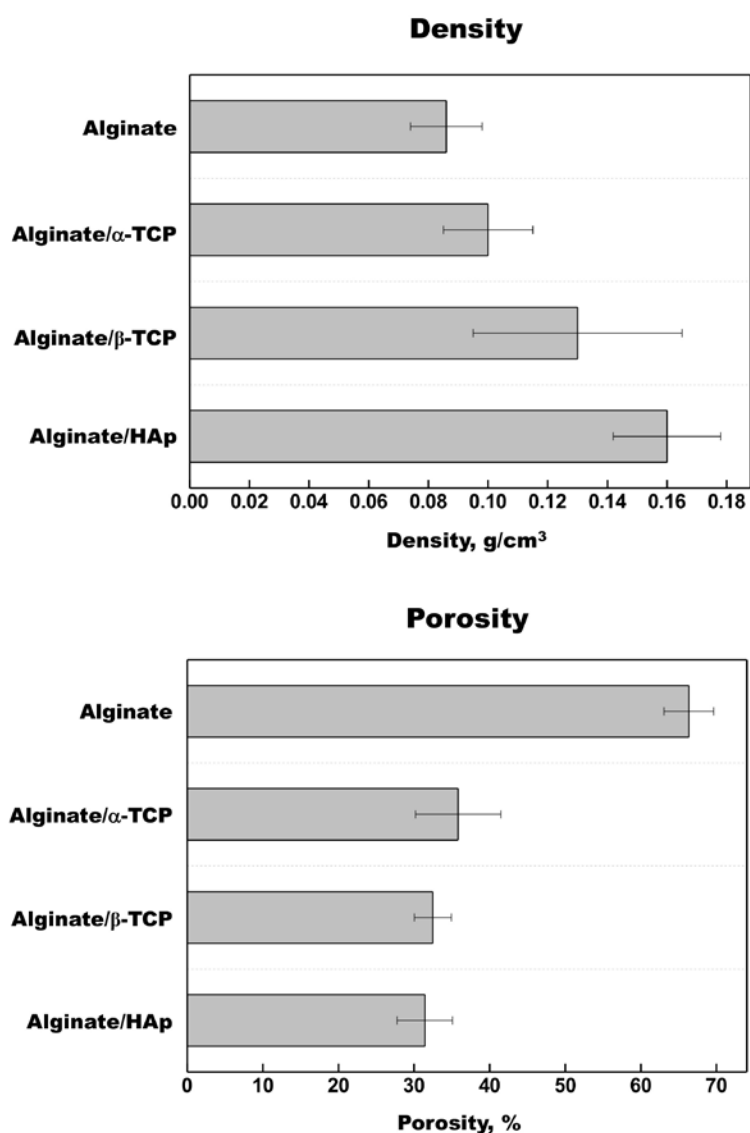


**Figure 5** Density and porosity of the prepared beads.

As a preliminary model of bioabsorption of the beads in an injection site, degradation was monitored *in vitro* by measuring the dry weight of the samples as a function of incubation time in saline at 37 °C (Fig. 6). Weight loss after 35 days decreased in the order: Alginate>Alginate/ $\beta$ -TCP>Alginate/ $\alpha$ -TCP>Alginate/HAp. The SEM images for the beads before and after immersion in PBS are shown in Fig. 7. Although a lot of pores were formed in Alginate after immersion, significant changes in size and shape were not observed. It was

found that addition of CaP to the alginate beads suppressed degradation in the aqueous environment, and this phenomenon would be induced by suppression of the swelling.

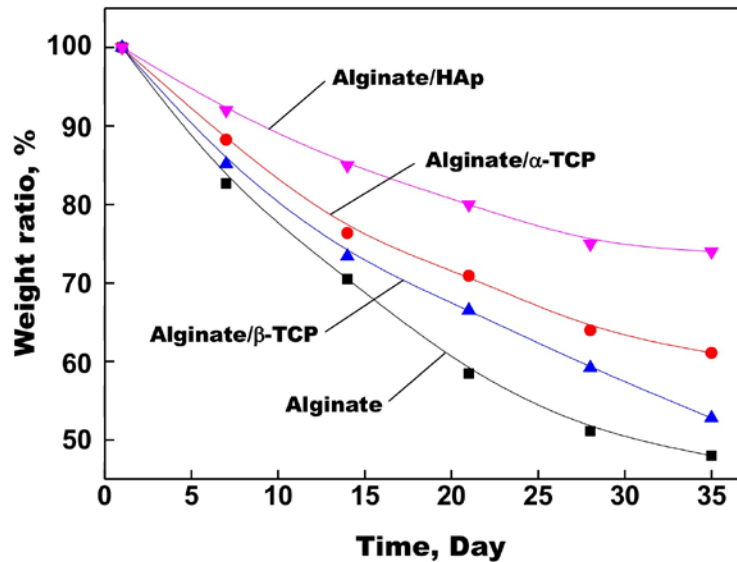


**Figure 6** Degradation rate *in vitro* of the prepared beads in a saline solution at 37°C for various time periods (n=4).

Blocks fabricated from each kind of beads were tested for their compressive strength (Fig. 8). Equal weights and volumes were maintained throughout the experiment to maintain the homogeneity of the system. The compressive strength of the blocks of Alginate, Alginate/ $\alpha$ -TCP, Alginate/ $\beta$ -TCP and Alginate/HAp were  $122.84 \pm 4.39$ ,  $125.52 \pm 11.2$ ,  $119.37 \pm 7.84$  and  $129.26 \pm 12.4$  MPa respectively.

Figure 9 shows the release profiles of methylene blue from the beads. Alginate showed a burst release profile. The  $t_{50}$  value (50% of drug release) for alginate was 55 minutes whereas the  $t_{50}$  values of the composite beads were extended to 100–300 minutes.

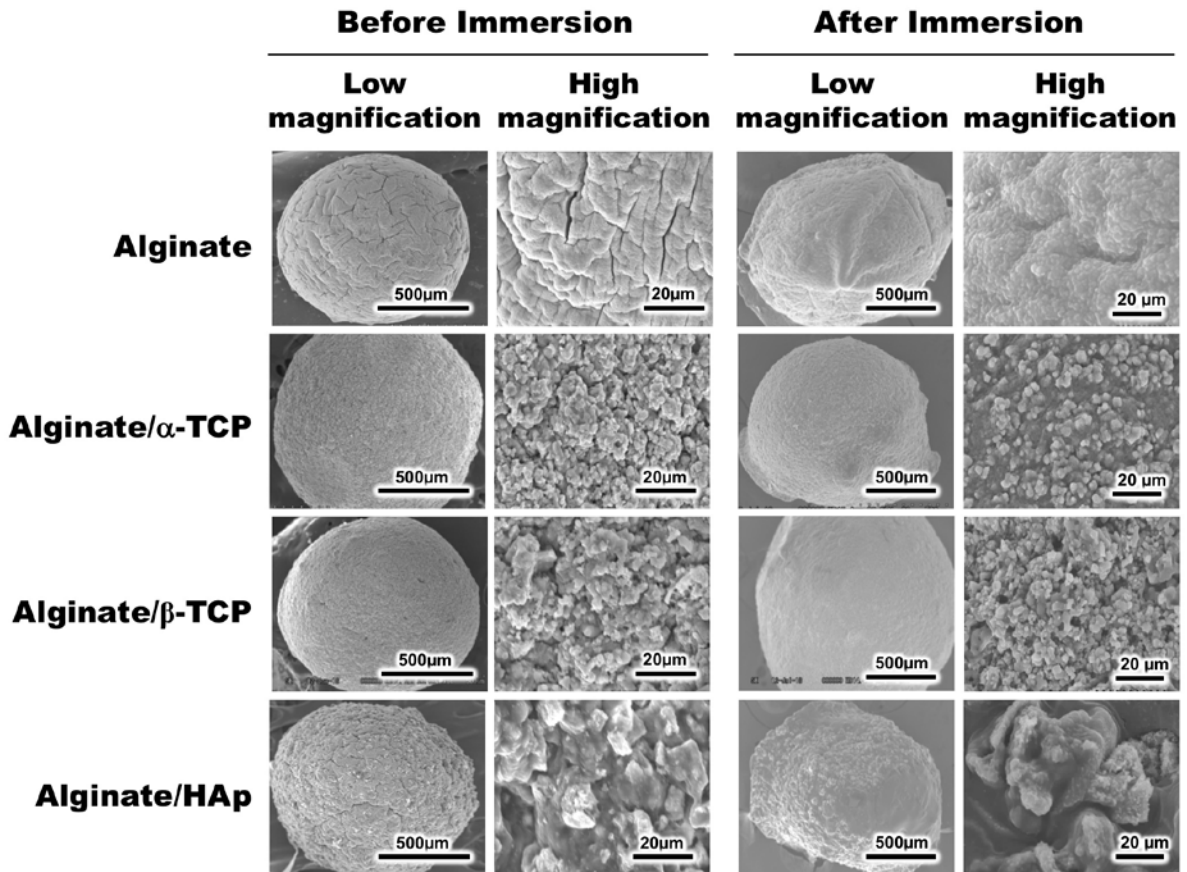


**Figure 7** SEM photographs of the prepared beads before and after immersion in saline at 37°C for 35 days.

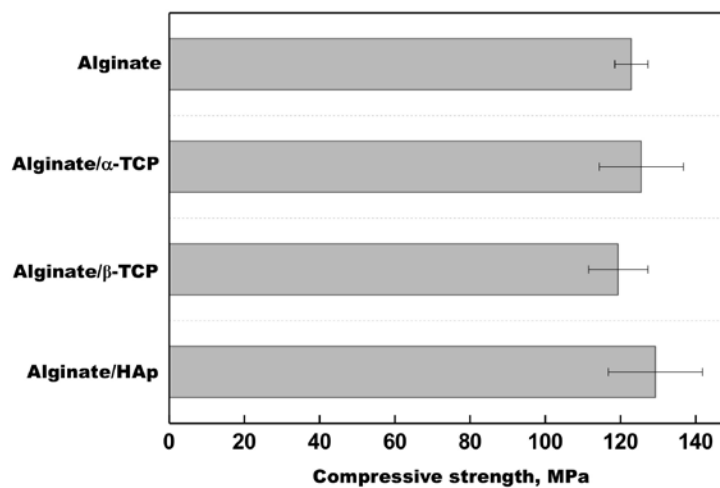


**Figure 8** Compressive strength of the blocks fabricated by accumulation of the prepared beads (n=8).

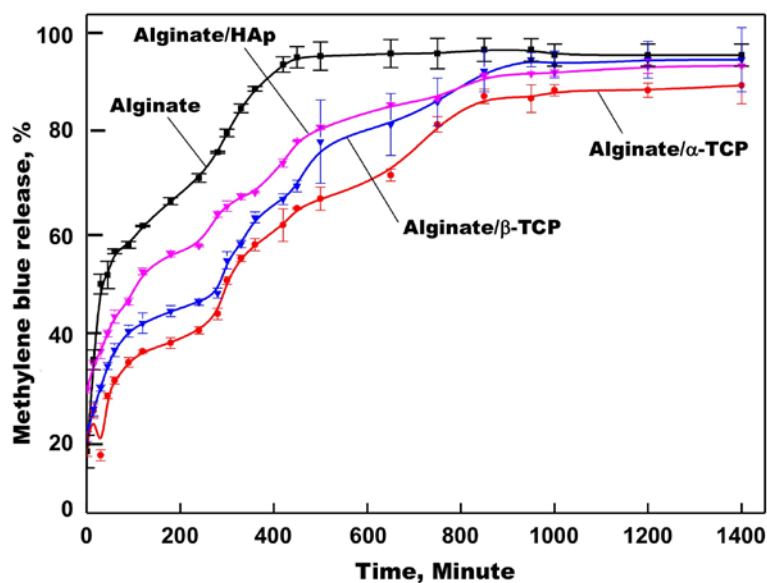


**Figure 9** *In vitro* release profiles of methylene blue from the prepared beads.

#### 4. Discussion

Composite microspheres of alginate and various CaP were prepared through gelation by  $\text{Ca}^{2+}$ . XRD results indicate that the amorphous nature of alginate is diminished by the accumulation of CaP particles (See Fig. 2). The crystallinity of each CaP was confirmed to remain intact in the ionically cross-linked polymer network, which may affect the mechanical properties of the hybrids.

Addition of HAp or  $\beta$ -TCP to the alginate microspheres decreased swelling ratio in aqueous conditions (See Fig. 4). In pure alginate, the large number of hydrophilic groups and the void space in the cross-linked network would lead to the highest swelling ratio. Addition of HAp or  $\beta$ -TCP to alginate beads was found to suppress the initial swelling in the aqueous environment. Ionic interactions between alginate and the added CaP would block significant water penetration. Meanwhile, Alginate/ $\alpha$ -TCP showed a similar swelling profile to alginate.  $\alpha$ -TCP could easily react with the surrounding water to convert into low crystalline HAp [31]. Therefore, a large amount of water could presumably penetrate into Alginate/ $\alpha$ -TCP. In the

case of Alginate/HAp, the swelling ratio significantly increased after 12 hours to resemble that of alginate. This could possibly be due to the degradation of the interface between alginate and HAp by the swelling, although detailed structural changes should be further analysed. Improvement of chemical bonding between alginate and HAp particles by silane coupling agents may suppress the significant swelling at the later stage.

Compressive strength of the blocks fabricated by accumulation of the microspheres was more than 100 MPa irrespective of inorganic phase (See Fig. 8). It is assumed that intergranular voids in the blocks are filled with polyacrylic acid even in pure alginate. The measured compressive strength of the hybrid blocks is comparable to that of typical glass ionomer cements [32]. Tanahashi *et al.* have demonstrated that carboxyl groups in organic polymers form tight ion-ion interactions with  $\text{Ca}^{2+}$  [33]. Therefore, similar interactions may exist between CaP and the carboxyl groups in alginate and/or the polyacrylic acid in the present samples. Blocks fabricated from the microbeads are thus expected to be useful materials for bone substitutes. For this purpose, not only compressive but also bending strength is important and it should be clarified in future. In order to enhance the bending strength, reinforcement of the interface between the constituent phases is important. In this study, ionic polyacrylic acid was used as a binder for fabrication of the blocks. This would enhance bonding of each microsphere, since components of the microspheres have also ionic characteristics.

It was found that incorporation of CaP into the alginate beads is effective for slow release of methylene blue (See Fig. 9) This can be attributed to the suppression of swelling and biodegradation (See Figs. 4 and 6). Moreover, CaP likely adsorbs methylene blue tightly onto their surfaces, having a larger quantity of ionic functional groups than alginate. Notably, the initial release rate of Alginate/HAp was higher than that of Alginate/ $\beta$ -TCP.  $\beta$ -TCP is reportedly more negatively charged than HAp [34], thus the former adsorbs the positively



charged methylene blue more tightly than the latter. This has implications in the selection of the appropriate kind of CaP according to the target drug to obtain the desired drug release profile.

In order to further understand the release behaviour, the release data were investigated by fitting the cumulative release data. Several mathematical equation models describe drug dissolution and/or release from DDS. In the modern era of controlled-release oral formulations, ‘Higuchi equation’ has become a prominent kinetic equation in its own right, as evidenced by employing drug dissolution studies that are recognized as an important element in drug delivery development [35]. After simplifying the above equation, Higuchi equation can be represented in the simplified form:

$$Q = K_H \times t^{1/2} \text{ -----(4)}$$

where  $K_H$  is the Higuchi dissolution constant.

The data obtained were plotted as cumulative percentage drug release versus square root of time. Therefore, the simple Higuchi model will result a linear  $Q$  versus  $t^{1/2}$  plot having gradient, or slope, equal to  $K_H$  and we say the matrix follows  $t^{1/2}$  kinetics.

For detailed kinetic study, we have selected the initial period drug release data from 5 to 120 minutes. The cumulative % drug release vs. square root of time graph has been plotted. As shown in Fig. 10, it is clear that all the set of prepared beads may follow the Higuchi square root model. It was noticed that higher correlation coefficient was observed in case of Alginate/ $\alpha$ -TCP and Alginate/HAp (0.99), but in case of Alginate and Alginate/ $\beta$ -TCP sphere it was 0.98. Hence, we can say that the drug release profile of methylene blue as model drug from the developed spheres mainly follows diffusion-controlled release mechanism at initial stage, although the mechanism may be changed later by partial degradation.

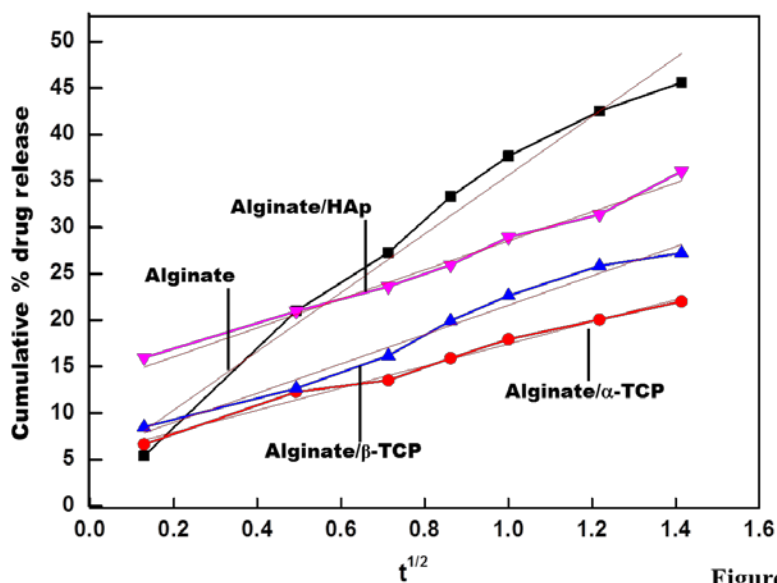


Figure 10

**Figure 10** Higuchi model kinetic release of methylene blue from prepared beads.

The obtained hybrid microspheres are expected to be applied for a drug delivery carrier. Many studies on *in vitro* and *in vivo* comparisons of drug release of polymer microspheres have been reported [36,37], but not many of inorganic materials. Wang *et al.* prepared microspheres with average particle size of 14.3  $\mu\text{m}$  in which the doxycycline was incorporated into poly(lactide-co-glycolide) (PLGA)-coated HAp microspheres, and compared their release behavior *in vitro* and *in vivo* [38]. The controlled release characteristics were improved by the PLGA coating. Furthermore, 40% of the contained doxorubicin was released in 150 h or more *in vitro*, and the steady concentration was maintained in mouse plasma. On the other hand, although the incorporated substances were different, the microspheres produced in this study released 40% of the methylene blue in 1 to 5 h. The main reason for these phenomena is thought to be the difference in hydrophobicity of the polymers. It is assumed that PLGA suppressed the penetration of the surrounding water

into the microspheres due to its hydrophobicity and contributed to the controlled release. In future study, control in the hydrophobicity of the polymers to optimize the drug release behavior is also needed.

## **5. Conclusions**

In this work, we performed a comparative study on alginate-based composite beads modified with various kinds of CaP. Particles with high sphericity were obtained irrespective of the kind of CaP. There were no significant differences in the mechanical behaviour of the blocks fabricated from the beads. The swelling properties and *in vitro* release profile of methylene blue differed between the beads of different CaP. The drug release profile of from the developed spheres is following diffusion-controlled release mechanism. The approach used in this study not only enhanced the bead strength substantially, but also prolonged the bead dissolution for controlled release of drugs. We have successfully demonstrated that microbeads with a suitable release profile for the target drug can be obtained by fabrication from alginate and the appropriate kind of CaP.

## **Acknowledgements**

The authors sincerely acknowledge Takeda Science Foundation for designating Dr. Garima Tripathi as Takeda Fellow and providing the financial support to carry out the research.

We thank Amy Tong from Edanz Group ([www.edanzediting.com/ac](http://www.edanzediting.com/ac)) for editing the English draft of this manuscript.

## **References**

1. Rush SM. Bone graft substitutes: osteobiologics. *Clinics in Podiatric Medicine and Surgery* 2005;22:619.
2. Verron E, Khairoun I, Guicheux J, Bouler JM. Calcium phosphate biomaterials as bone drug delivery systems: a review. *Drug Discov. Today* 2010;15:547.
3. Suchanek W, Yoshimura M. Processing and properties of hydroxyapatite-based biomaterials for use as hard tissue replacement implants. *J. Mater. Res.* 1998;13:94.
4. Ribeiro CC, Barrias CC, Barbosa MA. Preparation and characterisation of calcium-phosphate porous microspheres with a uniform size for biomedical applications. *J. Mater. Sci. Mater. Med.* 2006; 17:455.
5. Haddad AJ, Peel SA, Clokie CM, Sandor GK. Closure of rabbit calvarial critical-sized defects using protective composite allogeneic and alloplastic bone substitutes. *Craniofac. Surg.* 2006;17:926.
6. Luo Y, Lode A, Sonntag F, Nies B, Gelinsky M. Well ordered biphasic calcium phosphate–alginate scaffolds fabricated by multi-channel 3D plotting under mild conditions. *J. Mater. Chem. B* 2013;1:4088.
7. Zeng L, Yao Y, Wang DA, Chen X. Effect of micro cavitory alginate hydrogel with different pore sizes on chondrocyte culture for cartilage tissue engineering. *Mater. Sci. Eng.C* 2014;34:168.
8. Jin R, Teixeira LSM, Dijkstra PJ, Karperien M, van Blitterswijk CA, Zhong ZY, Feijen J. Injectable chitosan-based hydrogels for cartilage tissue engineering. *Biomaterials* 2009;30:2544.
9. Shen ZS, Cui X, Hou RX, Li Q, Deng HX, Fu J. Tough biodegradable chitosan–gelatin hydrogels via in situ precipitation for potential cartilage tissue engineering. *RSC Adv.* 2015;5:5640.

10. Luo Y, Shoichet MS. A photolabile hydrogel for guided three-dimensional cell growth and migration. *Nat. Mater.* 2004;3:249.
11. Mauck RL, Yuan X, Tuan RS. Chondrogenic differentiation and functional maturation of bovine mesenchymal stem cells in long-term agarose culture. *Osteoarthritis Cartilage* 2006;14:179.
12. Han L, Xu J, Lu X, Gan D, Wang Z, Wang K, Zhang H, Yuan H, Weng J. Biohybrid methacrylated gelatin/ polyacrylamide hydrogels for cartilage repair. *J. Mater. Chem. B* 2017;5:731.
13. Levingstone TJ, Matsiko A, Dickson GR, O'Brien FJ. A biomimetic multi-layered collagen-based scaffold for osteochondral repair. *Acta Biomater.* 2014;10:1996.
14. Miao T, Miller EJ, McKenzie C, Oldinski RA. Physically cross-linked polyvinyl alcohol and gelatin interpenetrating polymer network theta-gels for cartilage regeneration. *J. Mater. Chem. B* 2015;3:9242.
15. Levingstone TJ, Matsiko A, Dickson GR, O'Brien FJ. A biomimetic multi-layered collagen-based scaffold for osteochondral repair, *Acta Biomater.* 2014;10:1996.
16. Dai Y, Liu G, Ma L, Wang D, Gao C. Cell-free macroporous fibrin scaffolds for in situ inductive regeneration of full thickness cartilage defects. *J. Mater. Chem. B* 2016;4: 4410.
17. Puppi D, Chiellini F, Piras AM. Polymeric materials for bone and cartilage repair. *Prog. Polym. Sci.* 2010;35:403.
18. Sun J, Tan H. Alginate-Based Biomaterials for Regenerative Medicine Applications. *Materials* 2013;6:1285.
19. Lee GS, Park JH, Shin US, Kim HW. Direct deposited porous scaffolds of calcium phosphate cement with alginate for drug delivery and bone tissue engineering. *Acta Biomater.* 2011;7:3178.

20. Lee GS, Shin US, Park JH, Kim HW, Won JE. Alginate combined calcium phosphate cements: mechanical properties and in vitro rat bone marrow stromal cell responses. *J. Mater. Sci., Mater. Med.* 2011;22:1257.
21. Perez RA, Kim HW. Core-shell designed scaffolds of alginate/alpha-tricalcium phosphate for the loading and delivery of biological proteins. *J. Biomed. Mater. Res. A* 2013;101A:1103.
22. Perez RA, Kim JH, Buitrago JO, Wall IB, Kim HW. Novel therapeutic core-shell hydrogel scaffolds with sequential delivery of cobalt and bone morphogenetic protein-2 for synergistic bone regeneration. *Acta Biomater.* 2015;23:295.
23. Castilho M, Rodrigues J, Pires I, Gouveia B, Pereira M, Moseke C, Groll J, Ewald A, Vorndran E. Fabrication of individual alginate-TCP scaffolds for bone tissue engineering by means of powder printing. *Biofabrication* 2015;7: 015004.
24. Qiu X, Han Y, Zhuang X, Chen X, Li Y, Jing X. Preparation of nano-hydroxyapatite/poly(l-lactide) biocomposite microspheres. *J. Nanopart. Res.* 2007;9:901.
25. Lin LC, Chang SJ, Kuo SM, Niu GCC, Keng HK, Tsai PH. Preparation and evaluation of  $\beta$ -TCP/polylactide microspheres as osteogenesis materials. *J. Appl. Polym. Sci.* 2008;108: 3210.
26. Jung JP, Bhuiyan DB, Ogle BM. Solid organ fabrication: comparison of decellularization to 3D bioprinting. *Biomater. Res.* 2016;20: 27.
27. Galus S, Lenart A. Development and characterization of composite edible films based on sodium alginate and pectin. *J. Food Eng.* 2013;115:459.
28. Ma MG, Zhu YJ, Chang J. Monetite formed in mixed solvents of water and ethylene glycol and its transformation to hydroxyapatite. *J Phys Chem B* 2006;110:14226.
29. Carrodeguas RG, De Aza S.,  $\alpha$ -Tricalcium phosphate: synthesis, properties and biomedical applications. *Acta Biomater* 2011;7:3536.

30. Jin HH, Lee CH, Lee WK, Lee JK, Park HC, Yoon SY. In-situ formation of the hydroxyapatite/chitosan–alginate composite scaffolds. *Materials Letters* 2008;62:1630.
31. Monma H, Kanazawa T. The hydration of  $\alpha$ -tricalcium phosphate. *Yogyo-Kyokai-Shi* 1976;84: 209.
32. Bresciani E, Barata Tde J, Fagundes TC, Adachi A, Terrin MM, Navarro MF. Compressive and diametral tensile strength of glass ionomer cements. *J Appl Oral Sci.* 2004;12: 344.
33. Tanahashi M, Matsuda T. Surface functional group dependence on apatite formation on self-assembled monolayers in a simulated body fluid. *J Biomed Mater Res.* 1997;34: 305.
34. Lopes MA, Monteiro FJ, Santos JD, Serro AP, Saramago B. Hydrophobicity, surface tension, and zeta potential measurements of glass - reinforced hydroxyapatite composites. *J. Biomed. Mater. Res.* 1999;45:370.
35. Dash S, Murthy PN, Nath L, Chowdhury P. Kinetic modeling on drug release from controlled drug delivery systems. *Acta Pol. Pharm.* 2010;67:217.
36. Ishak RA, Mortada ND, Zaki NM, El-Shamy Ael-H, Awad GA. Impact of microparticle formulation approaches on drug burst release: a level A IVIVC. *J. Microencapsul.* 2014;31:674.
37. Shen J, Choi S, Qu W, Wang Y, Burgess DJ. In vitro-in vivo correlation of parenteral risperidone polymeric microspheres. *J. Control Release.* 2015;218:2.
38. Wang X, Xu H, Zhao Y, Wang S, Abe H, Naito M, Liu Y, Wang G. Poly(lactide-co-glycolide) encapsulated hydroxyapatite microspheres for sustained release of doxycycline. *Mater. Sci. Eng. B.* 2012;177:367.